



Universiteit
Leiden
The Netherlands

Hysterons and pathways in mechanical metamaterials

Ding, J.

Citation

Ding, J. (2023, May 31). *Hysterons and pathways in mechanical metamaterials*. *Casimir PhD Series*. Retrieved from <https://hdl.handle.net/1887/3619565>

Version: Publisher's Version

License: [Licence agreement concerning inclusion of doctoral thesis in the Institutional Repository of the University of Leiden](#)

Downloaded from: <https://hdl.handle.net/1887/3619565>

Note: To cite this publication please use the final published version (if applicable).

INTRODUCTION

1.1 Mechanical metamaterials

Mechanical metamaterials are materials with artificial structures designed such that the mechanical response differs from ordinary materials: it is the structure, not the composition, that is crucial [1–7]. In the past few decades, many surprising properties have been found in mechanical metamaterials.

A first example of such metamaterials are those with negative Poisson's ratio [1, 8, 9], also known as auxetic materials, which expand (contract) in the horizontal direction when stretched (compressed) in the vertical direction (Fig. 1.1a). In the simplest case, such an auxetic response already occurs in linear response, i.e. for infinitesimal deformations. To understand why a structured elastic material can have a completely different response than the constitutive material, consider the deformations in the metamaterial (Fig. 1.1a). Clearly in this case, the deformations are concentrated in narrow regions, near the tips of the beams — this inhomogeneity is crucial. It follows that slender structures, which concentrate deformations, are crucial for metamaterials. In fact, it can be shown that any physically sound elastic response can be encoded in the metamaterial structure [10].

Beyond linear response, one can harness elastic instabilities to obtain a nonlinear response, which allows to obtain switching and programmable functionalities [1, 2, 5]. A classic example of a switchable material are

made by patterning a thick slab of rubber with circular holes (Fig. 1b, see section 1.3). Under small vertical compression, the material deformations are mostly given by compression of the vertical slender elements in between the holes, and the material has a positive Poisson's ratio in linear response. However, for sufficiently strong compression, these slender elements buckle (see section 1.2) and the material undergoes a collective patterning instability, after which the material strongly contracts in the horizontal direction, thus featuring an effective negative Poisson's ratio [11]. This strategy can be extended by embedding frustration in the material to obtain programmable behavior. One example uses 'defects' in origami patterns to switch the material between different states with different stiffnesses [12]. Another example uses confinement by clamps to frustrate a hole-based metamaterial, leading to a programmable response where the materials switches between two differently buckled patterns under a vertical force depending on the confinement [2]. In general, the space of nonlinear mechanical metamaterials is much larger than that of linear ones, and is far from exhausted.

The examples above mostly focus on unusual values of common mechanical properties (stiffness, Poisson ratio). Increasingly, metamaterials with behavior that go beyond such properties have been realized. For example, most simple metamaterials feature a periodic array of unit cells, but by combining multiple unit cells, more complex functions can be designed. For example, stacking 3D building blocks in an aperiodic manner in such a way that all building blocks can deform smoothly, leads to textured metamaterials that can act as shapeshifters (Fig. 1.1c) [5]. These combinatorial designs can be extended to origami [13], to metamaterials with topological defects [6], and to a new class of oligomodal metamaterials [14].

A new theme is to study the sequential response of a mechanical metamaterial, as shown in Fig. 1.1d. For example, a self-folding metamaterial can be designed to undergo self-guided, multi-step reconfiguration under uniform compression [4]. A soft robotic hand constantly inflated at a constant velocity can bend its fingers in sequence [15]. A monolithic mechanical metamaterial is able to sequentially switch its pattern from a wavy shape to a diamond shape under tension [16]. The combination of spatial and

sequential complexity allows to blur the boundary between materials and devices; on the one hand, their behavior surpasses that of any other materials and cannot be expressed in ordinary material parameters — on the other hand, many of these materials remain functional when damaged or when cut in two parts, unlike ordinary devices. It is this class of ‘machine materials’ which form an important frontier for current research.

Sequential complexity in materials has as a consequence that the driving protocol starts to become important: instead of simply compressing a material, or perhaps using cyclic compression, more complex driving protocols (‘compress a bit, then decompress, then compress more, etc’) become of interest [17]. In particular, under cyclical driving, a multistable metamaterial produces sequential actions, depending not only on the amount of loading but also on the driving history of the sample [18] (Fig.1.4c). In this case, a frustrated system — related to crumpled paper — was found to exhibit complex orbits and in particular to distinguish between one or more driving cycles [18]. Moreover, cyclic extensions on a metamaterial consisting of a one-dimensional array of pre-curved beams can result in a sequence of contact formations and snapping of the beams, so that the material can ‘count’ and evolve between different states [19]. Another example explores cyclical inflating a system composed of bistable origami modules, also known as Kresling pattern [20] (Fig. 1.1e). Each surface of the classic, undeformed Kresling pattern is concave, as shown in the left three sub-figures in Fig. 1.1e. The surface is able to become convex when the sample is inflated until large pressure p_3^+ , and the surface will not become concave again until the sample is deflated to negative pressure p_3^- . By using different driving protocols, the system can reach multiple states at zero pressure [20] (Fig. 1.1e).

The central challenge in this thesis is to explore and characterize the sequential actions of complex metamaterials under cyclic driving, aiming at complex pathways, due to non-linear instabilities and multi-stability. This may impact our understanding of memory effects in materials [21] and ultimately may lead to programmable, smart metamaterials with a wide range of functionalities. In this thesis, we focus on bistable elements to create controllable sequential actions in an elastic system. We use 3D

printing to create our complex metamaterials, and study their response under cyclic driving. Crucial concepts, explained below, are the nonlinear instabilities (buckling and snapping) that we use (section 1.2); (bi)holey metamaterials that are the starting point of our studies (section 1.3), and pathways (section 1.4).

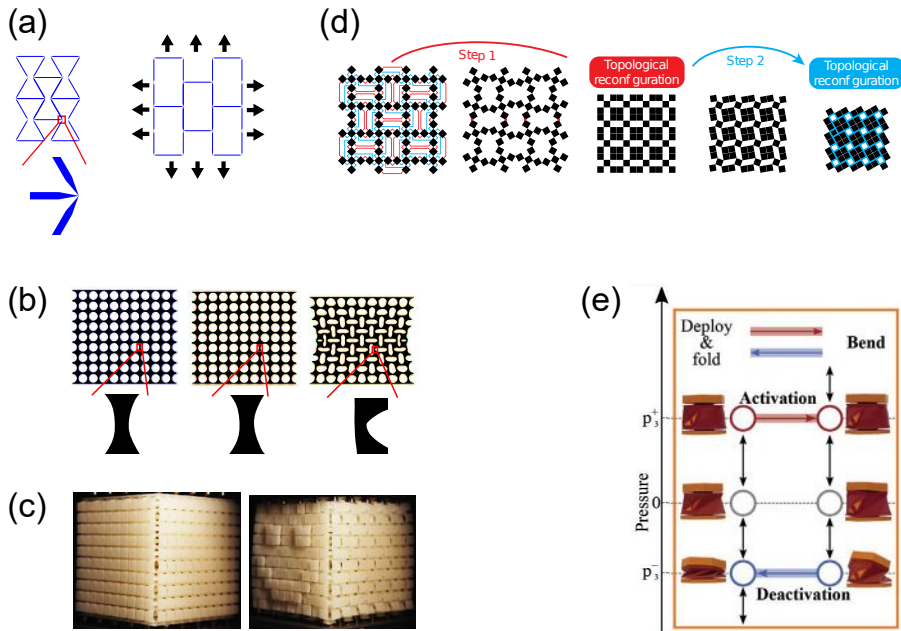


FIGURE 1.1: (a) An auxetic metamaterial expand in one direction when it is stretched in another direction. (b) A homogeneous holey metamaterial shows negative Poisson’s ratio under sufficiently strong compression. (c) A metacube that consists of precisely ordered building blocks shows a smiley face texture on its surface under compression [5]. (d) A mechanical metamaterial folds in two steps under monotonical driving [4]. (e) Creases on an origami modules can be actuated to obtain different configurations under the same pressure [20].

1.2 Buckling and snapping

Elastic instabilities result in non-linear behaviors of the stress-strain response of a system [1, 19, 22–32]. In particular, slender elements allowing large deformations are prone to instabilities, such as buckling and snap-through. In Chapters 2 to 4, we harness snapping events to design hysterons. In chapter 5, we discuss the buckling instability we observed in holey metamaterials. We now discuss the basic idea of buckling and snapping.

Buckling is a sudden change in shape of a slender ‘beam’ when it is under compressive load, such as a straight beam becoming curved under compression $\varepsilon := U/H$, where U is the amount of compression, H is the uncompressed height and ε is the strain. Elastic beams buckle when the external strain is larger than the critical strain ε_{cr} , and recover their initial shape when unloaded [1, 23, 25]. The buckling instability provides nonlinear but reversible building blocks for metamaterials, as shown in Fig. 1.2a.

Snap-through, also known as (un)snapping events, occur when a system quickly flips from one stable state to another stable state under a certain loading condition [1, 23, 25, 27–29]. Snapping often occurs in a multi-stable systems with confined boundary conditions and external loading, and is accompanied by hysteretic behavior. For example, a buckled beam can either curve to the left or the right, associated with two stable states, and is able to snap between these two states with external sideways pushing (Fig. 1.2b). The buckled beam can snap from its initial state to another stable state under external deflection loading ε^+ , and snap back with an opposite deflection loading ε^- . When $\varepsilon^+ > \varepsilon^-$, the beam is hysteretic. The driving force for snapping can also be applied to the boundaries of confinement [23, 33]. For example, rotating the boundaries of a curved beam can result in the beam snapping to another direction (Fig. 1.2b).

We harness these instabilities to create the non-linear response of metamaterials to uni-axial driving. A metamaterial usually consists of building blocks that are not perfectly straight beams, but the slender building blocks can nevertheless buckle or snap as well [1]. For example, a holey metamaterial consists of hourglass-shaped beams and diamond-shaped islands. The hourglass-shaped parts undergo a buckling instability when the metamaterial is compressed.

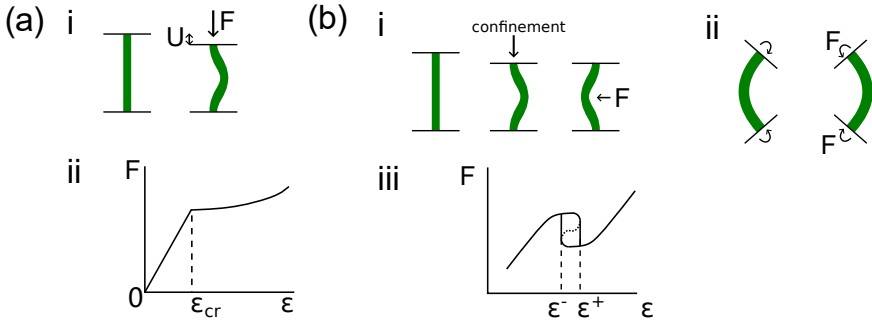


FIGURE 1.2: Instability of elastic beams. (a) Slender beam undergoes the buckling instability under uni-axial compression. (b) Constrained beams can snap to a different equilibrium state. Under displacement controlled driving, there is a hysteresis in the $F - \epsilon$ response, where ϵ denotes the dimensionless displacement of loading and F denotes the loading force. The dotted curve in panel (iii) denotes an unstable, experimental inaccessible branch.

1.3 Biholey metamaterials

A simple strategy to obtain mechanical metamaterials with a non-linear response is to pattern a thick slab of rubber with circular holes. In particular, when the rubber between the holes forms slender elements, the mechanical response becomes dominated by the buckling and bending of these slender elements. Here we focus on two well-studied geometries, featuring a square array of circular holes.

First, the homogeneous holey design consist of $m \times n$ circular holes of equal diameter D arranged in a square array (Fig. 1.3a). The pitch of the array is P , and the thickness of the thinnest part of the hourglass-shaped beam that separates the holes $t := P - D$. The sample usually will be compressed in the y -direction, and we number the holes by their x and y -positions as (i, j) ($0 < i \leq m, 0 < j \leq n$). The height $H \approx m \cdot P$ and width $W \approx n \cdot P$ describe the size of the patterned sample. The thickness of the sample in the third dimension, T , is chosen to prevent out-of-plane buckling in the experiment, while in simulation we use a 2D geometry. To ensure a homogeneous load, we extend the top and bottom parts by t_y . We consider the sample with two kinds of boundaries, which we refer to as side walls: the sample with side walls, as shown in Fig. 1.3a (i), is characterized by thickness of the edge beams, t_x , and the sample without side walls, as shown in Fig. 1.3a (ii), consists of half holes which are arranged in the same as the holes inside the sample.

Second, the biholey design consists of alternating larger and smaller holes of diameter D_1 and D_2 , separated by precurved, hourglass-shaped beams which are connected in groups of four in diamond shaped islands (Fig. 1.3b). Like the homogeneous holey array, each hole in biholar sample is labeled by (i, j) ($0 < i \leq m, 0 < j \leq n$), and each center of the hole is denoted by (x_i, y_j) .

As shown previously [2, 3, 11, 30, 34–39], compression of such samples yields a pattern of alternating horizontally and vertically oriented elliptical holes. We define the polarization of each hole as x -polarized or y -polarized. In metamaterials with equal hole sizes, the ensuing pattern is two fold degenerate — the polarization of a given hole is either vertical or horizontal, with neighboring holes having opposite polarization (see more in Chapter 6). In biholey systems, the symmetry between these two patterns is broken: the larger holes are vertically polarized under horizontal compression (Mode A) and horizontally polarized under vertical compression (Mode B). For monoholar samples, the onset of patterning occurs sharply at a critical compression strain, and is associated with a sharp kink in the force compression curve (Fig. 1.3c (i)). In contrast, the force response of a biholey

metamaterial to uni-axial compression is smooth, as shown in Fig. 1.3c, and the patterning is gradual.

Biholey metamaterials being compressed in both horizontal and vertical directions have been studied by Florijn et al[2, 3]. Their results show that the response to vertical compression can be programmed by horizontal confinement at a strain ε_x . This horizontal confinement is done by passive clamps, placed across the sample. Under vertical compression, a biholey metamaterial that is pre-confined by horizontal clamps shows four kinds of robust behavior. First, for very small confinement, the hole pattern smoothly deforms in mode B, and the force response F_y as well as the polarization of the holes Ω increase monotonically with compressive strain ε_y (regime *(i)* in Fig. 1.3d). Second, for small confinement, F_y exhibits a non-monotonic increase with ε_y featuring a range with negative incremental stiffness, and the hole pattern deforms smoothly between modes A and B (regime *(ii)* in Fig. 1.3d). Third, for moderate confinement, an instability arises, featuring $F_y - \varepsilon_y$ curve and $\Omega - \varepsilon_y$ curve exhibiting a clear hysteretic transition, and the hole pattern snaps between modes A and B. We note that the snapping strains can be programmed by the clamp sizes (regime *(iii)* in Fig. 1.3d). Last, for large confinement, the hole pattern smoothly deforms in mode A, and F_y increases monotonically with ε_y (regime *(iv)* in Fig. 1.3d).

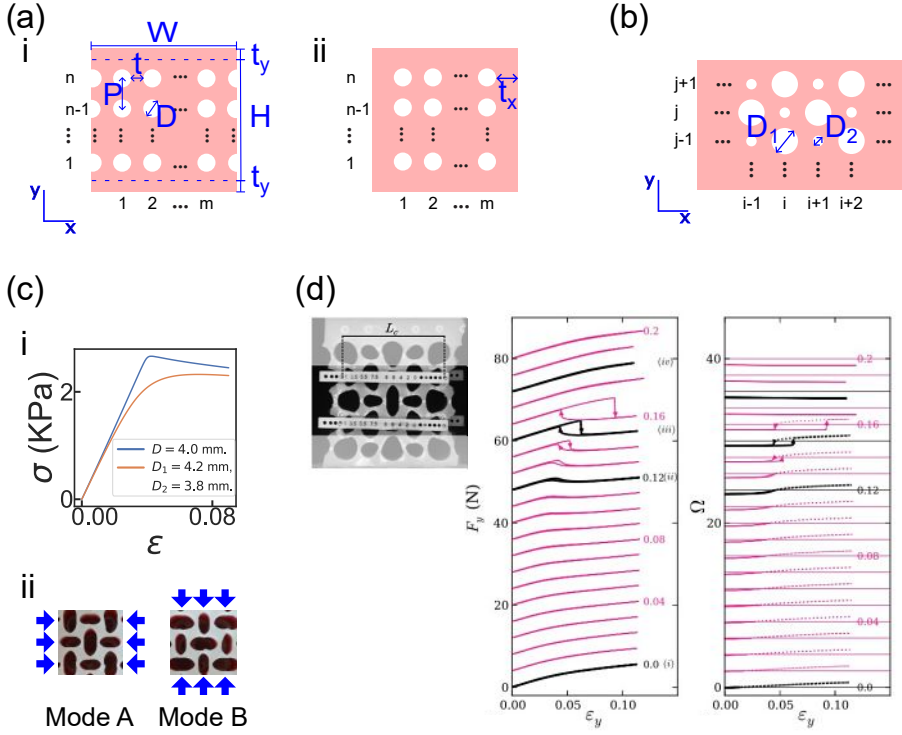


FIGURE 1.3: Hole metamaterial. (a) Example of homogeneous holey design. (b) Schematic of biholey design. (c) Response of holey metamaterial to uniaxial compression. (i) Numerical result of metamaterial with side walls 5×5 holes, where $P = 5$ mm and $t_x = t_y = 0$ mm. (ii) Biholey metamaterial shows a pattern of orthogonal ellipse. (d) Under vertical compression ϵ_y , the force response F_y and the polarization of the holes S of biholey metamaterial can be programmed by lateral confinement ϵ_x [2, 3]. The sample with 5×5 holes is characterized with $\{P, D\} = \{10 \text{ mm}, 7 \text{ mm}\}$. Curves are offset for clarity.

1.4 Pathways

Driven multistable metamaterials have shown complex pathways, featuring multi-step deformations [1–3, 5, 16, 33, 40–43]. These transition

pathways are hysteretic, and the visited states may depend on the global driving history. To characterize the memory effects of these transitions, we can collect the states and their transition pathways in a transition graph (t-graph) (Fig. 1.4a) [17, 18, 44–48].

It is often possible to model these states, as well as their hysteric transition pathways, by collections of hysterons. Hysteron flip their internal state s from '0' to '1' when the local driving exceeds the upper switching field ε^+ , and flip from '1' to '0' when the driving falls below the lower switching field ε^- (Fig. 1.4b) [17, 21, 44, 46, 47, 49]. Collections of uncoupled hysterons form the Preisach model [49], where the switching fields of a given collective state are associated with the switching field of the independent hysteron.

A currently emerging theme is coupled hysterons, where the values of the switching fields depend on all hysterons, i.e. the collective state $S := \{s_1, s_2, \dots\}$ [17, 18, 44–48]. Bense et al [18] show transition graphs of a curved, corrugated elastic sheet, where each groove of the sheet can either be in a snapped state or an un-snapped state, thus acting as a hysteron (Fig. 1.4c). The interactions between these hysterons allow a multitude of complex hysteron switching sequences, such as avalanche transitions, featuring multiple hysterons flipping together, and scrambled pathways, which feature pairs of transitions that are not consistent with a unique, state-independent ordering of the switching fields. Shohat et al [40] studied the interaction between hysterons modeled by the localized bistable wrinkles in an unfolded crumpled sheet. The result shows that the switching field of a hysteron is affected by its neighboring hysterons, which can either increase or decrease the switching field, thus evidencing hysteron interactions.

Our goal is to obtain samples with controlled complex pathways – for example, with different orderings for the snapping and un-snapping sequences – and to find design rules to control these pathways. We use different designs on hysterons, and investigate the method to tune the property of the hysterons, which allows tuning pathways. Moreover, we focus on the interaction between hysterons followed by non-trivial pathways. Our work shows that complex pathways can be realized experimentally in systems of interacting hysterons.

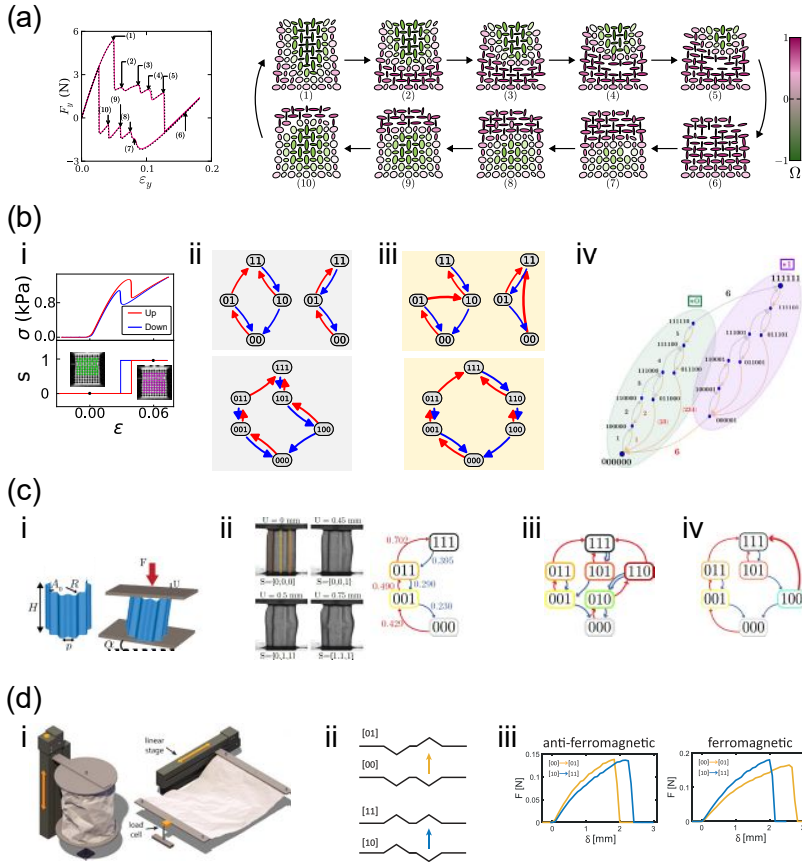


FIGURE 1.4: Cyclically driven metamaterials can feature memories in their collective states and transitions. (a) Example of force response and transition pathway of a multistable metamaterial [2, 3] showing that transition pathways are hysteric and the visited states depend on the global driving history. (b) Transition graphs showing the hysteric transition pathways and states of multistable metamaterials. (i) Under cyclic driving, a hysteron flips between '0' and '1' (Section 4.3). (ii) Examples of transition graphs of uncoupled hysteron [44]. (iii) Examples of transition graphs of coupled hysteron [44]. (iv) Transition graph that exhibits a hierarchy of cycles and subcycles [17]. (c) Transition graphs of a corrugated sheet under cyclical compression [18]. (i) Experiment setup. (ii) By tilting one of the driving plate, more states become accessible. Under cyclic compression, the sample shows four distinct mesostates, associated with the sudden snapping of different grooves. (iii) Scrambled graph, where the scrambled transitions are shown by double arrows. (iv) An avalanche transition appears which is shown by a bold arrow. (d) Interaction between hysteron [40]. (i) Experiment setup. (ii) Illustrations of the states of two neighboring hysteron, and two transitions $\{00\} \rightarrow \{01\}$ as well as $\{10\} \rightarrow \{11\}$. (iii) Examples of anti-ferromagnetic (ferromagnetic) interaction featuring flipping threshold for the right hysteron increases (decreases) when the left hysteron is flipped up.

1.5 Outline of the thesis

Chapter 2 discusses a method of creating mechanical hysterons, using a bistable beam. To create a bistable beam, we embed a defect beam in a biholey system. The defect beam features two distinct states – curving to the right and curving to the left — and is able to switch between these two states under cyclical compression. We start discussing the geometry of the defect as well as the simulation method. Next, we show the behavior of the defect — it can deform slowly and can deform dramatically. In particular, we discuss the examples where the defect act as a hysteron features two distinct states '0' and '1', and discuss the switching field between these states. Then we discuss why the defect is able to act as a hysteron. Finally, we discuss the design rules for creating controllable hysterons.

In Chapter 3, we embed a number of hysterons in a metamaterial, where the hysterons are able to flip in sequence under cyclic driving. Specifically, we use transition graphs to map the sequential behavior as well the state of the hysterons. First, we optimize the geometrical design of the defect compared to Chapter 2 so that the up and down switching fields can be tuned independently. Second, we show in detail the experimental approach to create hysterons, monitoring the hysterons, and controlling the switching field of a single hysteron. Third, we leverage gradients in the boundary conditions to tune the collective states and the transition pathways of the hysterons in a metamaterial. Finally, we show hidden degree of freedom of hysterons resulting from subtle frictional effects, which allows the switching fields to be modified by the driving history. Moreover, we map the evolution of the sample and hysterons to transition graphs that encode the pathways of a system.

In Chapter 4, we demonstrate a different strategy for creating hysterons, using a biholey metamaterial that features strong interactions. We leverage frustration between the configuration of the biholey pattern to horizontal and vertical compression. We start with the design of pre-clamped biholey metamaterial which acts as a group of hysterons under compression. We show that tuning the sizes of the clamps allows to access qualitatively differ-

ent pathways. Thirdly, we focus on the interaction between the hysterons, showing how switching fields of a hysteron depends on the collective state. In particular, we study avalanche transitions, featuring multiple hysterons flipping together, and explore their exotic behavior for a large variety of transition graphs.

In Chapter 5, we explore the deformation modes of monoholar metamaterials. First, we show that the spatial structure of the pattern forming deformation depends on whether the number of rows and columns is odd or even: for even numbers, the pattern breaks up into two or even four patches. Then we demonstrate the competition between these different patches, featuring snapping. We finally dope the sample with defects and show that these defects can be used to control the symmetry of the pattern forming deformation.